Impurity band structure of boron-doped homoepitaxial diamond

Takashi Inushima*
Department of Electronics, Tokai University, Hiratsuka 259-1292, Japan

Rinat F. Mamin
Kazan Physico-Technical Institute, Russian Academy of Science, Kazan 420029, Russia

Hiromu Shiomi
Sumitomo Electric Industries, Ltd., Koyakita, Itami, Hyogo 664-0016, Japan
(Received 25 September 2008; published 29 January 2009)

Impurity band structure of boron-doped diamond is investigated using $p^+/p^-/p^+$ mesa structures with thin p^- layers, where p^+ is heavily doped diamond with variable range hopping conductivity and p^- is less-doped diamond with valence-band conductivity. From the frequency and temperature dependence of the conductivity of the mesa structures, it is found that holes injected into the p^- layer stay at the $2p$ states of boron for an extremely long time and contribute to the conductivity. From the equivalent circuit analysis it is concluded that, when the boron concentration exceeds $\sim 4\times 10^{18}$ cm^{-3}, the $2p$ wave functions of boron begin to overlap, and an impurity band forms at $2p$ states, which is located ~ 0.07 eV above the valence-band maximum. Simultaneously, the Fermi level rises to the impurity band by a strong electron-optical phonon interaction and a variable range hopping is realized in this band.

DOI: 10.1103/PhysRevB.79.045210 PACS number(s): 72.20.Ee, 71.23.−k, 71.55.−i, 61.72.sh

I. INTRODUCTION

Since the discovery of superconductivity in boron-doped diamond,[1] its impurity band structure has been a key issue for the understanding of superconductivity. Though the impurity conduction has been thoroughly investigated since the 1950s,[2,3] the impurity band structure of diamond still remains in controversy.

It was first suggested that the impurity band forms at the lowest excited states of impurities,[4] but after Mott[5] formulated a concept of the impurity band analogous to the upper Hubbard subband, which was located U (the repulsion energy of electrons having opposite spins located on the same site) above the ground state of impurities, the idea of the lowest excited states was abandoned. Mott formulated two types of conductivity, impurity band conductivity with activation energy ϵ_2 at high temperatures and variable range hopping (VRH) conductivity by $\sigma(T)\propto\exp[-(T_0/T)^{1/4}]$ in the Anderson localized at low temperatures.[6] T_0 is the transition temperature from the former conductivity to the latter. In many reports the impurity conduction of p-type diamond is explained by the Mott concept, that is, VRH at the ground states of boron.[7–10] Now impurity band plays an important role in the explanation of the superconductivity of p-type diamond.[11,12]

Though this concept provides quite reasonable interpretations of many experimental data of Si and related semiconductors, there are several difficulties when it is applied to diamond. The most serious one is the observation of the VRH even at room temperature.[8–10,13,14] This causes the critical temperature $T_0\sim 10^4$ K,[10,13] which requires a broad impurity bandwidth of ~ 0.1 eV centered at the ground state of boron, and a short hopping distance of 3.5 Å. These conditions contradict the concept of VRH used in Si and Ge (Ref. 2). Another difficulty is the absence of ϵ_2. It is understood that when the impurity concentration is low, ϵ_2 is close to ϵ_1. When the concentration increases close to that of the Mott transition, ϵ_2 goes to zero.[2] In diamond, the change from ϵ_1 to ϵ_2 is not observed,[8,9,14] though it is obvious that there is a temperature region which shows two-band conduction.[7,9,15]

Homoepitaxial diamond growth technique provides us with samples with a smooth and clean interface so that we can fabricate thin diamond layers with an accurate impurity concentration with few trapping states at the interface.[16,17] Using this technique we fabricated $p^+/p^-/p^+$ mesa structure with thin p^- layer, where p^+ is heavily doped diamond with VRH and p^- is less-doped diamond with valence band conductivity. Its thermionic current showed that the Fermi level of the p^+ layer was ~ 0.05 eV above the valence band.[17] The capacitance versus voltage characteristics was explained by the formation of the depletion layer at the p^+ layer on the interface.[18]

In this paper, we focus on the holes injected into the p^- layer, which is meant for experimental verification of the Hubbard U mechanism in boron-doped diamond. By changing the p^- layer thickness and from the equivalent circuit analysis of the $p^+/p^-/p^+$ mesa structures, we determine that the impurity band is located at the lowest excited state of boron. Finally we discuss the boron concentration dependence of the Fermi level caused by a strong electron-optical phonon interaction, which is a developed idea from our previous work.[19] The impurity band structure at the lowest excited states of boron will help to explain the superconductivity of boron-doped diamond.

II. EXPERIMENTAL DETAILS

The homoepitaxial films used in this experiment were grown on off-orientated substrates [(001) substrates with a 7° off-angle toward ⟨110⟩] of polished Ib-synthesized diamond by microwave-enhanced chemical-vapor deposition

 ©2009 The American Physical Society

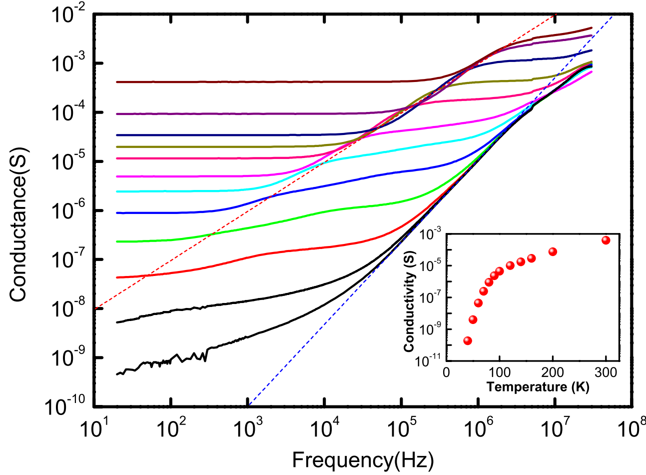

FIG. 1. (Color online) Frequency dependence of the conductance of the mesa structure with a p^- layer thickness of 70 nm. The measuring temperatures are from bottom to top, 40, 50, 60, 70, 80, 90, 100, 120, 140, 160, 200, and 300 K, respectively. Inset shows the dc conductance of the mesa structure (σ_{dc}). Dotted lines in the figure show $\sigma(\omega) \propto \omega^{1.0}$ and $\omega^{1.8}$ dependence.

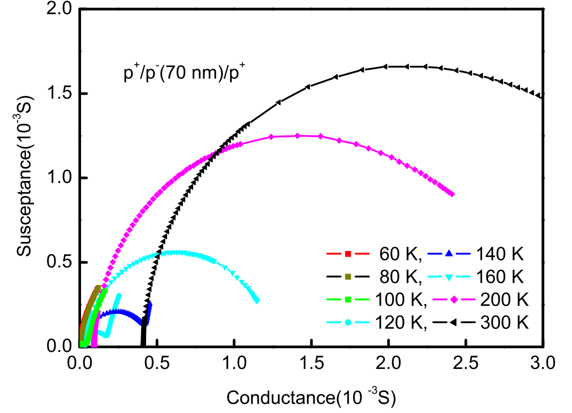

FIG. 2. (Color online) Cole-Cole plot of the mesa structure with a p^- layer thickness of 70 nm.

(CVD).[20] B_2H_6 was used as a doping gas and the ratio of B_2H_6/CH_4 is used to identify the samples' ppm in this paper. There is a clear change in conductivity from the valence band to VRH when the boron concentration $(N_B) \simeq 4 \times 10^{18}$ cm^{-3}.[15] In this experiment, 5000 ppm of the B_2H_6/CH_4 ratio corresponds to $N_B = 2 \times 10^{19}$ cm^3.[21]

In order to verify the Hubbard U mechanism, we fabricated $p^+/p^-/p^+$ mesa structures by the method reported before, where p^+ is 5000 ppm boron-doped diamond having a VRH conductivity and p^- is 500 ppm boron-doped diamond having a valence-band conductivity.[18] The p^- layer thickness was chosen to be 70 nm and 35 nm for the evaluation of the lifetime of carriers injected into the layer.

It is reported that metal-semiconductor (M-S) transition occurs at a hole concentration (n_h) of $\sim 2 \times 10^{20}$ cm^{-3}.[7,13,22] The maximum n_h in our samples is 3.5×10^{19} cm^{-3} (5000 ppm), which is an order of magnitude smaller than that for M-S transition.

III. RESULTS

The capacitance and conductance of the mesa structure strongly depend on frequency and temperature. Figure 1 shows the frequency dependence of the conductance $G(\omega)$ of the mesa structure with a 70-nm-thick p^- layer measured at an amplitude of 0.01 V. At the zero-frequency limit, $G(\omega)$ approaches σ_{dc}, whose temperature dependence is shown in the inset of Fig. 1. From the Arrhenius plot of σ_{dc}, an activation energy of ~ 0.06 eV is obtained below 80 K, which is the energy difference between the valence band and the Fermi level of the p^+ layer. This value is in good agreement with that obtained from the thermionic current measurement at 40 K.[17]

As is shown in Fig. 1, $G(\omega)$ depends on ω in four steps. The first step is observed in the low-frequency region where $\sigma(\omega)$ is constant against the ω change, then the second step appears, where $G(\omega)$ is expressed by $\omega^{1.0}$ for three decades of ω at 140 K. The $\omega^{1.0}$ dependence is reported to be the result of nearest neighbor hopping (NNH) mechanism between the occupied and unoccupied states in boron-doped Si.[23] The third step is the second plateau, and $G(\omega)$ becomes almost constant against the ω change again. The fourth is the part where $\sigma(\omega) \sim \omega^{1.8}$, which is observed up to the highest frequency region.

The frequency dependence of $G(\omega)$ through the second to the third steps can be understood to be caused by the transition current in the p^- layer, and the Cole-Cole plot of the conductance $G(\omega)$ versus susceptance $\omega C(\omega)$ gives us the temperature dependence of the carrier relaxation in the p^- layer, which is shown in Fig. 2. The plots produce semicircles with the centers on the conductance axis, which indicates that there is a single relaxation process in the p^- layer and is expressed by the Debye equation

$$\epsilon(\omega) = \epsilon_\infty + \frac{\epsilon_s - \epsilon_\infty}{1 - i\omega\tau_0}. \quad (1)$$

In Eq. (1), ϵ_∞ and ϵ_s are the high-frequency and the static dielectric constants, respectively, and τ_0 is the relaxation time of the carriers in the p^- layer. The radius of the semicircles becomes smaller as the temperature decreases and vanishes below 90 K.

As the p^- layer thickness reduces to half (35 nm), the current passing through the p^- layer becomes larger and the four steps observed in the ω dependence of $G(\omega)$ becomes unclear. The Cole-Cole plot of this structure shown in Fig. 3, however, indicates that there is a single relaxation process above 140 K, because the centers of the semicircles lie on the conductance axis. Hence, the carriers injected into the 35-nm-thick p^- layer also have relaxation given by Eq. (1).

In Eq. (1), τ_0 is obtained at the inverse of ω_0 where the susceptance becomes the maximum. Thus determined τ_0 is plotted as a function of inverse temperature in Fig. 4, where both of the τ_0's of Fig. 2 and 3 are plotted. These τ_0's are on a straight line with an activation energy (E_T) of 0.06 eV.

The hole injected from the valence band into the p^- layer is regarded as a hole trapped in a well with a potential barrier E_T and has a probability of jumping up to the valence band.

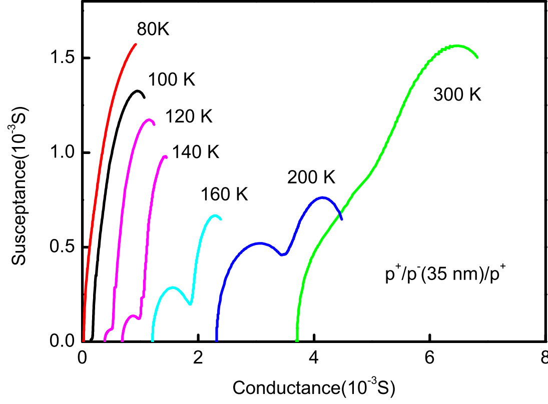

FIG. 3. (Color online) Cole-Cole plot of the mesa structure with a p^- layer thickness of 35 nm.

In this case, according to the elementary kinetic theory, the probability α of the hole per unit time is

$$\alpha = \Gamma \exp\left(\frac{-E_T}{kT}\right), \tag{2}$$

where Γ is a constant, and $\Gamma = kT/2\pi\hbar$ according to Eyring's reaction rate theory. Since there is only one relaxation process in the p^- layer, $\tau_0 = 1/\alpha$ is satisfied and the injected hole has a barrier height of $E_T = 0.06$ eV. When we use the Eyring's Γ, $\tau_0 = 5 \times 10^{-10}$ s at 100 K, which is 10^{-6} shorter than that shown in Fig. 4. Hence the injected hole stays for an extremely long time in the p^- layer. Our results confirm the report of Nebel *et al.*[24] that the injected carrier staying at an excited state has an extremely long lifetime in $4 \sim 8 \times 10^{18}$ cm^{-3} boron-doped diamond.

Figure 4 shows that there is a trap level in the p^- layer 0.06 eV above the valence band. This energy is similar to the energy difference between the $2p$ states of boron impurity and the valence-band maximum, and is also very close to that observed as the band offset energy at the p^+/p^- interface.[17] As the p^- layer does not have such a level in the bulk, the trap level at 0.06 eV in the p^- layer is only applicable to the hole injected from the valence band. In other words, the injected hole does not fall to the ground state of boron but stays at the excited level. This is because the Fermi level of the p^- layer is located much higher than the ground state of borons which are fully occupied by their own holes.

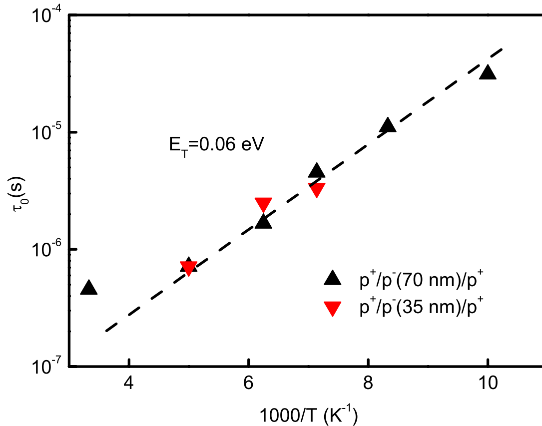

FIG. 4. (Color online) Temperature dependence of the relaxation time τ_0 given by Eq. (2).

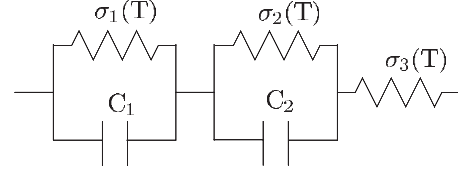

FIG. 5. Equivalent circuit for the $p^+/p^-/p^+$ mesa structure.

Glesener[25] presented a carrier capture model on the basis of deep level transient spectroscopy and said that when a carrier in the valence band is captured by an impurity, it occupies the highest excited states of the acceptor and then quickly tunnels to the lowest excited level. At the lowest excited level (E_T=82 meV), the trapped hole is either thermalized back to the valence band or falls down to the ground states via a slow multiphonon decay. His equation gives $\tau_0 = 1.5 \times 10^{-6}$ s at 300 K, which is similar to our result shown in Fig. 4. According to his results, the carrier-capture cross section is 4×10^{-13} cm^2, which corresponds to the Bohr radius of the lowest excited level of impurity boron (3.7 nm). Therefore the $2p$ excited states are the most probable candidate for the virtual trap level in the p^- layer.

An alternative possibility of E_T is A^+ states which are positively charged by extra holes. The formation of an isolated A^+ ion requires an activation energy which is equal to the ionization energy less hole affinity of an isolated neutral acceptor. This activation energy is lowered by the resonance energy as a result of the interaction between the A^+ states. But as will be seen in Sec. IV, the Fermi level of 5000 ppm diamond is almost the same as E_T of 500 ppm diamond, suggesting that the interaction energy is negligible. Moreover, it is difficult to observe activation energy ϵ_2 in the temperature dependence of the conductivity,[14] indicating that the trap level caused by A^+ states does not exist.

IV. EQUIVALENT CIRCUIT ANALYSIS

In this section we will analyze the frequency dependence of $G(\omega)$ and $C(\omega)$ of the mesa structure using a simple equivalent circuit. As there are two capacitors in the mesa structure as seen in Figs. 2 and 3, we apply the equivalent circuit shown in Fig. 5. The left part is an *R-C* network of the p^- layer with a single Debye relaxation process. The center part has another *R-C* network which governs the thermionic current between p^+ and p^- interfaces. The right part is the conduction of the bulk. Using $G(\omega)$ and $C(\omega)$, the admittance $Y(\omega)$ of the equivalent circuit is expressed as follows:

$$Y(\omega,T) = G(\omega,T) + i\omega C(\omega,T)$$
$$= \left[\frac{1}{\sigma_1(T) + i\omega C_1} + \frac{1}{\sigma_2(T) + i\omega C_2} + \frac{1}{\sigma_3(T)}\right]^{-1},$$

$$\sigma_1(T) = \sigma_{10}e^{-\epsilon_{10}/kT} + \sigma_{11}e^{-\epsilon_{11}/kT},$$

$$\sigma_2(T) = \sigma_{20}e^{-\epsilon_{20}/kT},$$

TABLE I. Summary of the fitting parameters used for equivalent circuit analysis.

d_1 (nm)	C_1 (pF)	C_2 (pF)	σ_{10} (S)	σ_{11} (S)	σ_{20} (S)	σ_{30} (S)	ϵ_{10} (eV)	ϵ_{11} (eV)	ϵ_{20} (eV)	ϵ_{30} (eV)
35	2000	10	0.3	1.3×10^{-3}	0.5	0.007	0.07	0.001	0.07	0.003
70	420	10	6.3×10^{-3}	6.3×10^{-7}	0.275	0.0012	0.07	0.001	0.07	0.003

$$\sigma_3(T) = \sigma_{30}e^{-\epsilon_{30}/kT}. \quad (3)$$

Here $\sigma_1(T)$ is the conductance of the p^- layer that consists of two parts having different activation energies ϵ_{10} and ϵ_{11}. ϵ_{10} is observed for the carriers injected into the p^- layer and it should be the same as E_T. ϵ_{11} is observed at low temperature when the injected carrier is transferred by a tunneling mechanism into the p^- layer. $\sigma_2(T)$ is the conductance associated with the p^+/p^- interface and has a barrier height of $\sim$0.05 eV(ϵ_{20}) as was found from thermionic current measurements.[17] $\sigma_3(T)$ is the conductance of the bulk part (p^+ layer) and has an activation energy of ϵ_{30}. This part shows a weak temperature dependence ($\sim$3 meV) and is the most conductive among the three components [$\sigma_3(T) \gg \sigma_1(T),\sigma_2(T)$].

In the equivalent circuit, d_1 is the thickness of the p^- layer (d_1=70 and 35 nm), d_2 and d_3 are those of the p^+ layers (d_2=1.6 μm, d_3=4.6 μm), the electrode area S is 0.78 mm^2, and the dielectric constant ϵ=5.7. C_1 is the capacitor of the p^- layer equal to $\epsilon S/d_1$, then $C_1 \simeq 550$ pF for d_1=70 nm and $\simeq$1100 pF for d_1=35 nm. C_2 is the capacitor associated with the electrodes on the p^+ layer and $C_2 = \epsilon S/(d_2+d_3)$, then $C_2 \simeq 6$ pF. Starting with these initial values, we reproduced $G(\omega)$ of Fig. 1 and obtained the circuit parameters given in Table I.

Using these values the temperature dependence of σ_{dc}, G(100 kHz), and C(100 kHz) can be reproduced as shown in Fig. 6. The equivalent circuit reproduces the experimental data quite well.

In Fig. 7 the temperature dependence of $G(\omega)$ with the 35-nm-thick p^- layer is shown together with the calculated $G(\omega)$ using the parameters given in Table I. For the fitting, the activation energies are fixed at the same values as those of d_1=70 nm. When d_1 becomes half, the mesa structure becomes more conductive and large C_1, σ_{10}, and σ_{11} are obtained, which suggests that the actual d_1 might be much smaller than 35 nm. Temperature dependence $\sigma(\omega)$, however, can be reproduced well, indicating that the equivalent circuit model qualitatively explains the electronic structure of the mesa structure.

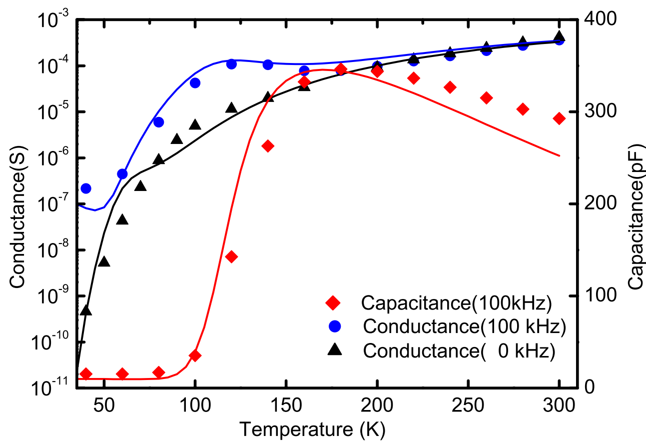

FIG. 6. (Color online) Temperature dependence of C(100 kHz), G(100 kHz), and σ_{dc} of the d_1=70 nm mesa structure. The fitting curves are obtained using the circuit shown in Fig. 5. The parameters of the circuit are given in Table I.

From the equivalent circuit analysis we conclude that there is a barrier height of 0.07 eV at the p^+/p^- interface, which indicates that the Fermi level of the p^+ layer is fixed at 0.07 eV (ϵ_{20}) above the valence band below 90 K. The carriers injected into the p^- layer stay 0.07 eV (ϵ_{10}) above the valence band virtually. The fact that ϵ_{10} is equal to ϵ_{20} indicates that the virtual trap level in the p^- layer is the lowest excited state of boron and has the same origin as the hopping band in the p^+ layer.

V. DISCUSSION

In textbooks, impurity conduction is thought to take place in an impurity band illustrated as B in Fig. 8(a), where the band is separated from the valence band and split by Hubbard U from the lower Hubbard band denoted by A.[2] The position of the Fermi level depends on the degree of compensation. Owing to the random fields of the charged donors, the states in the lower Hubbard band are Anderson localized and not full, and the Fermi level lies in band A (E_{F1}). When the temperature is high, conduction is governed by the carriers excited from the Fermi level to the mobility edge (E_M) in band B, and N_B dependent ϵ_2 is observed as an activation

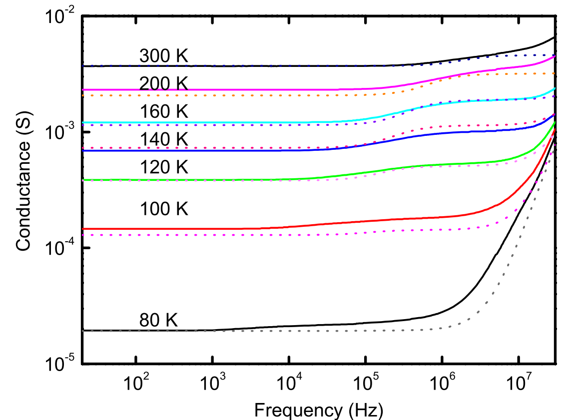

FIG. 7. (Color online) Temperature dependence of $G(\omega)$ with d_1=35 nm. The fitting curves are obtained using the circuit shown in Fig. 5. The parameters of the circuit are given in Table I.

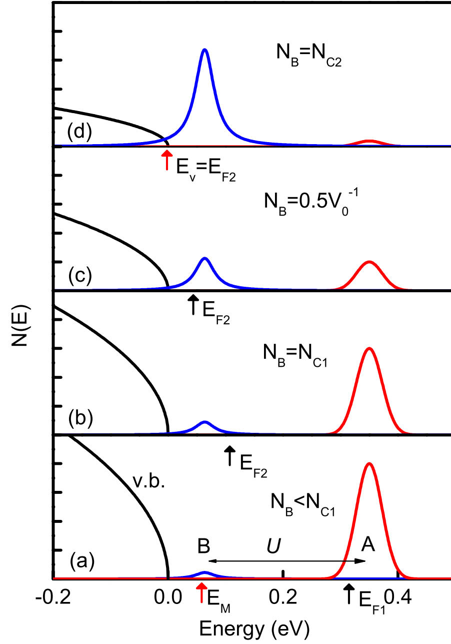

FIG. 8. (Color online) Boron concentration (N_B) dependence of the impurity band structure in diamond. Band A forms at the boron ground states and band B at the $2p$ excited states. E_{F1} and E_{F2} are Fermi energy positions. N_{c1} and N_{c2} are the critical densities for the change in the conduction (see text). The impurity band structure given in Ref. 2 is shown in (a); A and B are Hubbard bands and are split by Hubburd U. E_M is the position of the "mobility edge."

energy. When the temperature is low, conduction is realized by the hopping of carriers to the nearest available empty site at E_{F1} within band A (VRH). As the impurity concentration increases, bands A and B merge into one and the Mott transition occurs.

Since the impurity band model given in Fig. 8(a) does not explain the temperature dependence of the conductivity and Hall coefficients of heavily boron-doped diamond, we presented an idea of additional states of the impurity located 0.07 eV above the valence band.[19] For the formation of the additional states, interaction between nearest-neighbor atoms such as *B-B*, *B-C-B*, *B-C-C-B*, *B-N-B*, and *B-N-C-B* was assumed in high concentration of impurities.

The results shown in Fig. 4 suggest that the virtual trap state in the p^- layer has the same origin as the impurity band in the p^+ layer, and it is the lowest excited state of boron. Then, the previous scenario has to be modified as follows. When N_B is small, boron atoms are isolated from each other and each has one hole. As N_B increases, electron-phonon interaction at the boron sites intensifies because the hole in the ground state and the optical phonon have the same symmetry of Γ'_{25} at the Γ point[26] and the Bohr radius of the $1s$ wave function a is similar to the lattice constant d of diamond. It is well known that electron-phonon coupling is strongest at $a \sim d$ because the localized electron interacts most effectively with phonons whose wavelength $(2\pi/q)$ is comparable to the orbital radius a, whereas the phonon frequency spectrum has its peak at $q \sim \pi/d$ near the zone boundary.[27]

The conduction mechanism drastically changes at $N_{c1} = 4 \times 10^{18}$ cm^{-3} (N_B=1000 ppm), hence the average distance between borons at N_{c1} is estimated using $r_{c1} = (4\pi N_{c1}/3)^{(-1/3)}$, and $r_{c1} \approx 4$ nm is obtained. This value is close to that of the reported cross section of the $2p$ wave function (3.7 nm),[25] suggesting that the $2p$ wave function starts to overlap with that of the neighboring boron atoms at N_{c1}.

When the $2p$ wave functions overlap, two holes are shared by two borons as the result of the strong electron-phonon interaction. Then among the N_B holes, N_1 holes are at the ground state A (E_1=0.37 eV) and N_2 holes are at the lowest excited state B (E_2=0.07 eV). The number of N_2 is estimated by statistical law: $N_2 = N_B^2 V_0$ ($V_0 \simeq 5$ nm^3 is the volume of the interacting area). This scenario works well when the spin-triplet (Hund triplet) state is more stable than the spin-singlet state expected in the Hubbard U mechanism. In the Hund triplet state, the extra hole has the $2p$ orbital. Since the calculated U is higher than the $2p$ excited energy,[8] or the hole correlation is strong enough, the holes in singlet states are unstable and relax to the lowest excited level. Moreover, the $2p$ state is energetically favorable for the holes to hop over the boron impurities.

As N_B increases, the density N_2 increases very quickly and when the number of N_2 exceeds the number of donors N_D, which cannot be excluded in the plasma CVD process, the Fermi level jumps from E_{F1} to E_{F2} as shown in Fig. 8(b). This mechanism is essentially the same as that used for the calculation of the temperature dependence of the Fermi level of boron-doped diamond.[19] The critical concentration N_{c1} is obtained from the relation $N_1 = N_B - N_D$, which leads to $N_{c1} = (N_D V_0^{-1})^{1/2}$. Hence N_{c1} depends on N_D or on the degree of compensation $K = N_D/N_B$. When we use $V_0 = 5$ nm^3 and $K \simeq 0.02$, $N_{c1} \simeq 4 \times 10^{18}$ cm^{-3} is obtained.

When $N_B > N_{c1}$, the density of states A and B becomes equal at $N_B = 0.5V_0^{-1}$ when $K \simeq 0$ [Fig. 8(c)]. An M-S transition is expected to occur when the Fermi level reaches the top of the valence band, $E_{F2} = E_v$, as shown in Fig. 8(d). Thus we get critical $N_B = N_{c2}$ from

$$N_{c2} = \int_{E_v}^{\infty} N(E) dE + N_D. \tag{4}$$

From numerical calculation $N_{c2} \sim 1-5 \times 10^{20}$ cm^{-3} is obtained. When $N_B = V_0^{-1}$ all borons are in the interacting states and $N_B = N_2$. $V_0^{-1} = 2 \times 10^{20}$ cm^{-3} is the boron concentration reported for M-S transition.[13]

The mobility edge is at the top of the valence band in our model, which is denoted as E_v in Fig. 8(d). Then the conductivity is explained in terms of the holes conducting in the valence band and hopping in band B. As this process works in a wide temperature range, ϵ_2 is not observed.

The scenario presented here explains the N_B dependence of the absorption spectra reported before. When the boron concentration is low, the prominent absorption peaks are at 0.305 and 0.347 eV, which are the transitions from $1s$ to optically forbidden $2P_1$ and optically allowed $2P_2$ states, respectively.[14] These transitions form a sharp Gaussian shape, accompanied by LO-phonon sidebands in the higher energy region. The phonon sidebands intensify with the increasing boron concentration. When N_B exceeds N_{c1}, the ab-

sorption spectrum changes into a Lorentzian shape governed by the single absorption at 0.35 eV, and the fine structure disappears, which indicates a drastic decrease in the relaxation time of the excited carriers or an appearance of the impurity band at N_{c1}.

Recently the electronic structure of metallic and nonmetallic boron-doped diamond was studied by x-ray absorption and emission spectroscopy.[28] The impurity state ascribed to boron was observed near the Fermi level, which was at the top of the nondoped diamond. These results confirm the impurity band structure we presented in Fig. 8(d).

VI. SUMMARY

Impurity band structure of boron-doped diamond is investigated using $p^{+}/p^{-}/p^{+}$ mesa structures with thin p^{-} layers, where p^{+} is heavily doped diamond with impurity band conductivity and p^{-} is less-doped diamond with valence-band conductivity. When the boron concentration exceeds $\sim 4 \times 10^{18}$ cm^{-3}, an impurity band forms not at A^{+} states expected by Mott, but at the lowest $2p$ levels of the impurity boron, which is located ~ 0.07 eV above the valence-band maximum. Mechanism of impurity band formation was discussed based on strong hole-optical phonon interaction and hole-hole correlation. When the wave functions of $2p$ states of boron start to overlap with each other, the Fermi level rises to the $2p$ states and a variable range hopping is realized in this band in a wide temperature range.

ACKNOWLEDGMENT

The authors gratefully acknowledge the support from the Grant-in-Aid for Scientific Research Grant No. 19560321 of the Japan Society for the Promotion of Science.

*inushima@keyaki.cc.u-tokai.ac.jp

[1] E. A. Ekimov, V. A. Sidorov, E. D. Bauer, N. N. Mel'nik, N. J. Curro, J. D. Thompson, and S. M. Stishov, Nature (London) **428**, 542 (2004).
[2] N. F. Mott and E. A. Davis, *Electronic Processes in Non-crystalline Materials* (Clarendon, Oxford, 1979).
[3] B. I. Shklovskii and A. L. Efros, *Electronic Properties of Doped Semiconductors* (Springer-Verlag, New York, 1984).
[4] E. M. Conwell, Phys. Rev. **103**, 51 (1956).
[5] N. F. Mott, Can. J. Phys. **34**, 1356 (1956).
[6] N. F. Mott, J. Non-Cryst. Solids **1**, 1 (1968).
[7] A. W. S. Williams, E. C. Lightowlers, and A. T. Collins, J. Phys. C **3**, 1727 (1970).
[8] B. Massarani, J. C. Bourgoin, and R. M. Chrenko, Phys. Rev. B **17**, 1758 (1978).
[9] M. Werner, R. Job, A. Zaitzev, W. R. Fahrner, W. Seifert, C. Johnston, and P. R. Chalker, Phys. Status Solidi A **154**, 385 (1996).
[10] T. Sato, K. Ohashi, H. Sugai, T. Sumi, K. Haruna, H. Maeta, N. Matsumoto, and H. Otsuka, Phys. Rev. B **61**, 12970 (2000).
[11] G. Baskaran, Sci. Technol. Adv. Mater. **7**, S49 (2006).
[12] T. Shirakawa, S. Horiuchi, Y. Ohta, and H. Fukuyama, J. Phys. Soc. Jpn. **76**, 014711 (2007).
[13] T. Klein *et al.*, Phys. Rev. B **75**, 165313 (2007).
[14] A. Ogasawara, T. Inushima, T. Shiraishi, S. Ohya, S. Karasawa, and H. Shiomi, Diamond Relat. Mater. **6**, 835 (1997).
[15] T. Inushima, A. Ogasawara, T. Shiraishi, S. Ohya, S. Karasawa, and H. Shiomi, Diamond Relat. Mater. **7**, 874 (1998).
[16] H. Shiomi, Y. Nishibayashi, and N. Fujimori, Jpn. J. Appl. Phys., Part 1 **30**, 1363 (1991).
[17] T. Inushima, T. Matsushita, S. Ohya, and H. Shiomi, Diamond Relat. Mater. **9**, 1066 (2000).
[18] T. Inushima, T. Matsushita, R. Mamin, S. Ohya, and H. Shiomi, Appl. Phys. Lett. **77**, 1173 (2000).
[19] R. F. Mamin and T. Inushima, Phys. Rev. B **63**, 033201 (2001).
[20] H. Shiomi and Y. Kumazawa, Diamond Films Technol. **6**, 95 (1996).
[21] H. Shiomi, Y. Nishibayashi, N. Toda, and S. Shikata, IEEE Electron Device Lett. **16**, 36 (1995).
[22] E. Bustarret, E. Gheeraert, and K. Watanabe, Phys. Status Solidi A **199**, 9 (2003).
[23] M. Pollak and T. H. Geballe, Phys. Rev. **122**, 1742 (1961).
[24] C. E. Nebel, E. Rohrer, and M. Stutzmann, J. Appl. Phys. **89**, 2237 (2001).
[25] J. W. Glesener, Appl. Phys. Lett. **64**, 217 (1994).
[26] M. I. Eremets, Semicond. Sci. Technol. **6**, 439 (1991).
[27] S. Nakajima, Y. Toyozawa, and R. Abe, *The Physics of Elementary Excitations* (Springer-Verlag, Berlin, 1980).
[28] J. Nakamura, E. Kabasawa, N. Yamada, Y. Einaga, D. Saito, H. Isshiki, S. Yugo, and R. C. C. Perera, Phys. Rev. B **70**, 245111 (2004).